

# Effects of Content on the Electrochemical Characteristics of Nano-Structure Controlled Ti-alloys

M.Y. Oh\*, H.C. Choe\*, Y.M. Ko\*, S. J. Park\* and W.Brantley\*\*

College of Dentistry, Chosun University, 2<sup>nd</sup> Stage of Brain Korea 21 for College of Dentistry, Gwangju, Korea, [hcchoe@chosun.ac.kr](mailto:hcchoe@chosun.ac.kr)

\*\* College of Dentistry, Ohio State University, Columbus, OH, USA

## ABSTRACT

The purpose of this study was to develop new dental Ti-Zr alloys having an excellent mechanical properties, good corrosion resistance and biocompatibility. Microstructure properties and corrosion resistance obtained the as-cast and homogenized Ti-xZr alloys were useful for application to biomaterial.

Ti-Zr (10, 20, 30 and 40 wt%) alloys were prepared by arc melting and nano-structure controlled for 24 hr at 1000 °C in argon atmosphere. Phase constitutions and micro-structure of the specimens were characterized by X-ray diffractometer(XRD), optical microscopy(OM) and scanning electron microscopy(SEM). The corrosion properties of the specimens were examined through potentiodynamic test, potentiostatic test in artificial saliva solution by potentiostat (EG&G Co, PARSTAT 2273. USA). In as-cast and homogenized Ti-xZr alloys,  $\alpha$ -phase was identified by XRD. Microstructures were changed from lamellar structure to needle-like structure as Zr content increased.

From the results of corrosion resistance in the Ti-xZr alloys, corrosion resistance was increased as Zr content increased. Consequently, in the Ti-xZr alloys, surface stability for biomaterials increased as Zr content increased.

**Keywords:** Zr content, electrochemical characteristic, nano-structure, Ti-alloys

## 1 INTRODUCTION

Titanium alloys are expected to be much more widely used for implant materials in the medical and dental fields because of their superior biocompatibility, corrosion resistance and specific strength compared with other metallic implant materials. The use of titanium and its alloys implant applications has mainly been limited to the alloy Ti-6Al-4V and to cp-titanium [1, 2]. For medical application titanium and Ti-6Al-4V have been used since 1960s, with Ti-6Al-4V gradually replacing cp-titanium due to the increased mechanical strength of plates, nails, screws and endoprostheses [3].

Recently, however, much concern has developed over the issue of biocompatibility with respect to the dissolution of aluminum and vanadium ions and the possibility of any toxic effects [4-6]. Consequently, other titanium alloys are

currently being considered as alternatives to the Ti-6Al-4V alloy. Therefore, Ti-alloy, Al and V free and composed of non-toxic element such as Nb and Zr as biomaterials has been developed. Especially, Zr element belongs to same family in periodic table as Ti element. Addition of Zr to Ti alloy has an excellent mechanical properties, good corrosion resistance, and biocompatibility [7].

In order to investigate the effects of content on the electrochemical characteristics of nano-structure controlled Ti-alloys for biomaterials have been researched using by electrochemical methods.

## 2 EXPERIMENTAL

### 2.1 Alloy preparation.

Ti (G&S TITANIUM, Grade. 4, USA) alloys containing Zr (Kurt J. Lesker Company, 99.95 % wt% in purity) up to 10, 20, 30 and 40 wt% were melted six times to improve chemical homogeneity using the vacuum arc melting furnace. And heat treatment was carried out at 1000°C for 24h in order to homogenization in argon atmosphere.

The specimens for electrochemical test were prepared by using various grit emery papers and then finally, polished with 0.3  $\mu\text{m}$  Al<sub>2</sub>O<sub>3</sub> powder. All of polished specimen was ultrasonically cleaned and degreased in acetone.

### 2.2 Phase constitution and microstructure analysis.

Microstructures of the alloys were examined by optical microscopy (OM, OLYMPUS BM60M) and scanning electron microscopy (SEM, HITACHIS-3000). The specimens for the OM and SEM analysis were etched in Keller's solution consisting of 2 ml HF, 3 ml HCl, 5 ml HNO<sub>3</sub> and 190 ml H<sub>2</sub>O.

In order to identify the phase constitutions of the Ti-xZr alloys, X-ray diffraction (XRD) analysis with a Cu-K  $\alpha$  radiation were performed.

### 2.3 Electrochemical test.

Electrochemical characteristics were performed in a standard three-electrode cell having specimen as a working electrode and a high dense carbon as counter electrode.

The potential of working electrode was measured against a saturated calomel electrode (SCE) and all given potentials were referred to this electrode.

The corrosion properties of the specimens were examined through potentiodynamic test (potential range of -1500 ~ 2000 mV), potentiostatic test (const. potential of 300 mV) at scan rate of 1.67 mV/sec in artificial saliva solution at 36.5±1 °C by potentiostat (EG&G Co, PARSTAT 2273. USA). The chemical compositions of artificial saliva solution were given in Table 1.

After electrochemical corrosion tests, the surfaces of each specimen were investigated by using SEM (scanning electron microscopy)

Table1: Composition of artificial saliva.

NaCl	0.4 g
KCl	0.4 g
CaCl · 2H <sub>2</sub> O	0.906 g
NaH <sub>2</sub> PO <sub>4</sub> · 2H <sub>2</sub> O	0.690 g
Na <sub>2</sub> S · 9H <sub>2</sub> O	0.005 g
Urea	1.0 g
Distilled Water	1000 ml

### 3 RESULTS AND DISCUSSION

#### 3.1 Phase constitutions and microstructure

The X-ray diffraction patterns of as-cast and heat treatment for 24h at 1000 °C in argon atmosphere Ti-xZr(10, 20, 30, and 40 wt%) alloy are shown in Figure 1. From the results of X-ray diffraction patterns, the  $\alpha$ -phase peak was observed only in as-cast and heat treated Ti-xZr alloy. It suggested that  $\beta \rightarrow \alpha$  transformation progressed gradually with increasing Zr content due to Zr displacement[8]. Each diffraction peak shifted to a lower angle with increasing Zr content. The absence of additional peaks is consistent with single-phase.

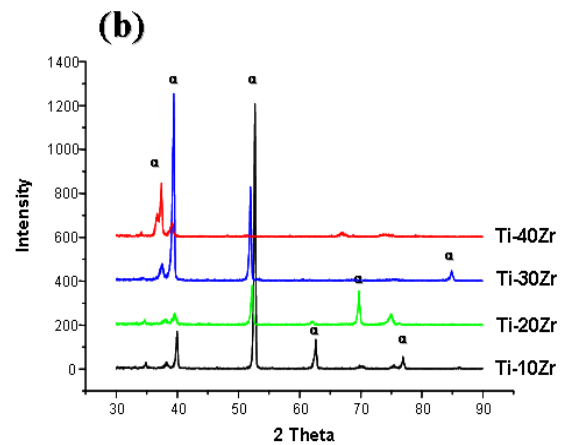
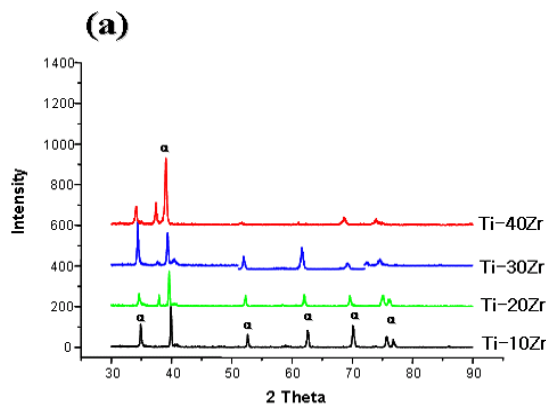


Figure 1: X-ray diffraction patterns of Ti-xZr alloys. (a) as-cast (b) homogenized

Figure 2 and 3 show microstructures of Ti-xZr alloys with different Zr contents. In the Figure 3 and 4,  $\beta$ -phase appeared dark part and  $\alpha$ -phase was bright part[9]. The microstructures of Ti-10Zr and Ti-20Zr alloy showed lamellar structure and needle-like structure, these phase changed gradually to almost needle-like structure in Ti-40Zr alloy. Consequently, microstructures of Ti-xZr alloys were changed from lamellar structure to needle-like structure as Zr content increased.

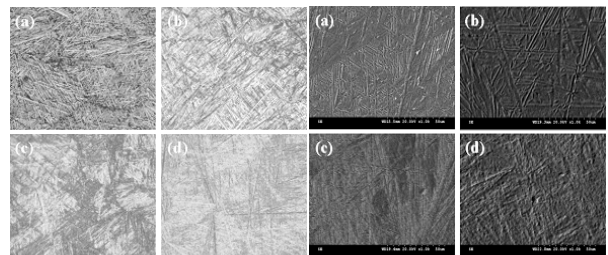


Figure 2: OM, SEM micrographs of as-cast Ti-xZr alloys. (×200) (a) Ti-10Zr (b) Ti-20Zr (c) Ti-30Zr (d) Ti-40Zr

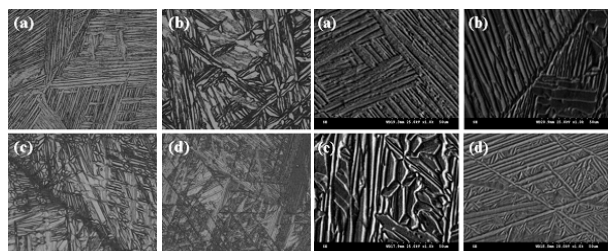


Figure 3: OM and SEM micrographs of homogenized Ti-xZr alloys. (×200) (a) Ti-10Zr (b) Ti-20Zr (c) Ti-30Zr (d) Ti-40Zr

### 3.2 Electrochemical characteristics

Figure 4 shows the results of potentiodynamic test (potential range of  $-1500 \sim 2000$  mV) in artificial saliva, which was conducted in order to investigate the effect of Zr content on the polarization curve. From the results of polarization behavior, Zr addition effect on polarization behavior did not show in the as-cast Ti-xZr alloys due to heterogeneous of cast structure, but it found that the corrosion resistance was increased with increasing Zr content, in the homogenized Ti-xZr alloys. It is thought that increase of corrosion resistance with Zr content is attributed to the a few nm thick passive film such as  $\text{TiO}_2$  and  $\text{ZrO}_2$  formed[10, 11] rapidly on the specimen surface. A few nm thick passive films could restrict the movement of metal ions from the metal surface to the solution, thus minimizing corrosion [12]. Corrosion current density ( $I_{\text{corr}}$ ) and corrosion potential ( $E_{\text{corr}}$ ) of Ti-xZr alloys after electrochemical test in artificial saliva solution at  $36.5 \pm 1^\circ\text{C}$ , as given in Table 2. It was confirmed that  $I_{\text{corr}}$  decreased and  $E_{\text{corr}}$  increased as Nb content increased in Ti-xZr alloys from Table 2.

Table 2: Corrosion current density ( $I_{\text{corr}}$ ) and corrosion potential ( $E_{\text{corr}}$ ) of Ti-xZr alloys after electrochemical test in artificial saliva solution at  $36.5 \pm 1^\circ\text{C}$

	As-cast				Homogenized			
	Ti-10Zr	Ti-20Zr	Ti-30Zr	Ti-40Zr	Ti-10Zr	Ti-20Zr	Ti-30Zr	Ti-40Zr
$E_{\text{corr}}$ (mV)	-910	-790	-970	-710	-900	-950	-860	-810
$I_{\text{corr}}$ ( $\text{A}/\text{cm}^2$ )	$3.358 \times 10^{-7}$	$2.861 \times 10^{-7}$	$8.436 \times 10^{-7}$	$3.493 \times 10^{-7}$	$1.880 \times 10^{-7}$	$1.508 \times 10^{-7}$	$1.307 \times 10^{-7}$	$7.702 \times 10^{-8}$

Figure 5 shows the results of potentiostatic test (const. potential of 300 mV) in artificial saliva solution at  $36.5 \pm 1^\circ\text{C}$  by potentiostat (EG&G Co, PARSTAT 2273, USA).

From results of passivation stability test, current density of homogenized specimen ( $7.702 \times 10^{-8} \text{ A}/\text{cm}^2$ ) showed lower than that of as-cast specimen ( $3.483 \times 10^{-7} \text{ A}/\text{cm}^2$ ) with 1-order difference. Current density of Ti-40Zr decreased with increasing corrosion time. Generally, when current density ( $I_{\text{corr}}$ ) in passive region get lower, amount of ion release through the passive film is small due to formation of thick passive film such as  $\text{TiO}_2$  and  $\text{ZrO}_2$ [10]. Therefore, pitting corrosion resistance is better [13].

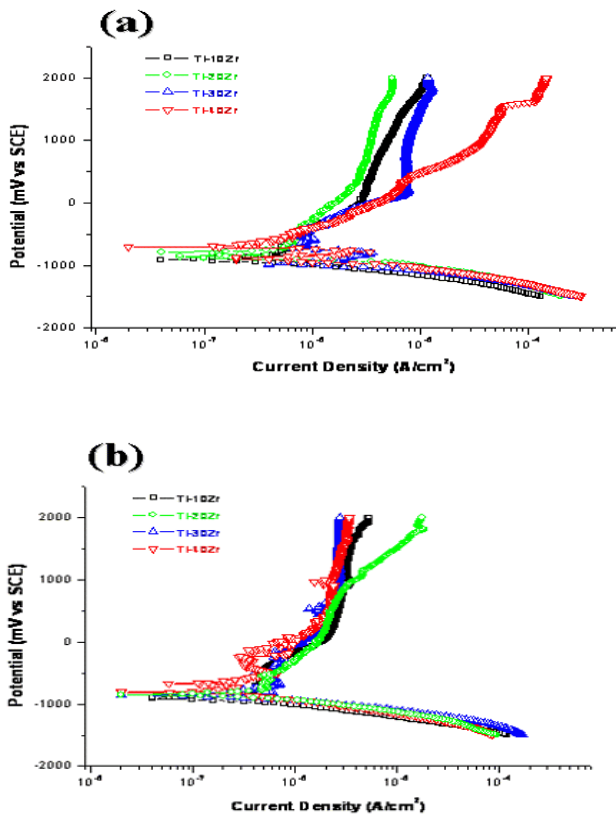


Figure 4: The polarization curves of Ti-xZr alloys after potentiodynamic test in artificial saliva solution at  $36.5 \pm 1^\circ\text{C}$ . (a) as-cast (b) homogenized

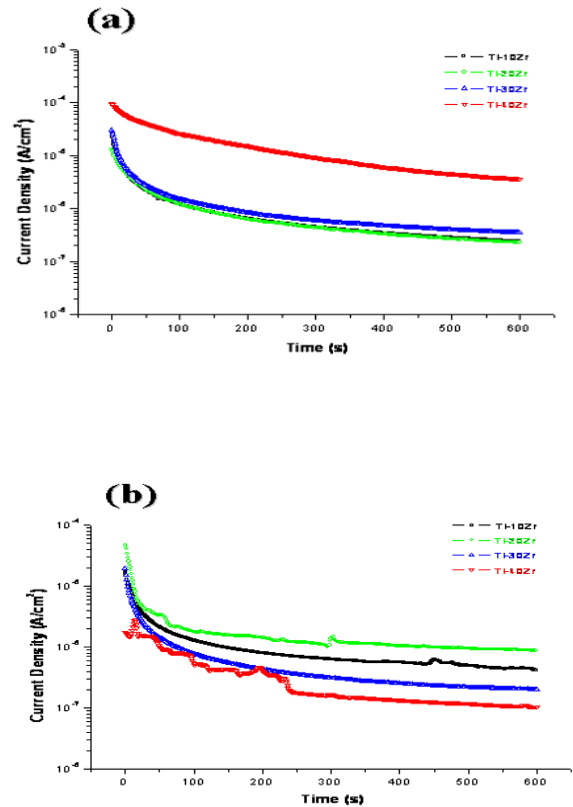


Figure 5: Current density-time curves (const. 300 mV) of Ti-xZr alloys after potentiostatic test in artificial saliva solution at  $36.5 \pm 1^\circ\text{C}$ . (a) as-cast (b) homogenized

Figure 6 shows corrosion micrographs of surface for as-cast and homogenized Ti-xZr alloys after potentiodynamic test in artificial saliva solution at  $36.5 \pm 1^\circ\text{C}$ . The corrosion attack by  $\text{Cl}^-$  ion appeared in grain boundary and  $\beta/\alpha$ -interface[6] of both as-cast and homogenized Ti-xZr alloys as shown in Figure 6.

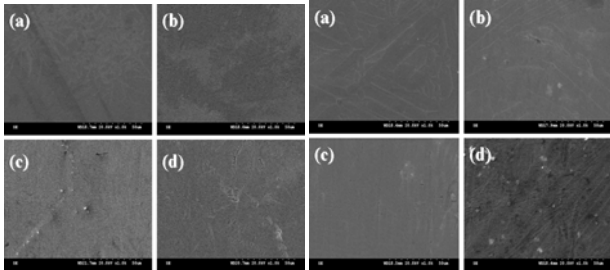


Figure 6: SEM micrographs of surface for as-cast and homogenized Ti-xZr alloys after potentiodynamic test in artificial saliva solution at  $36.5 \pm 1^\circ\text{C}$ . (a) Ti-10Zr (b) Ti-20Zr (c) Ti-30Zr (d) Ti-40Zr

#### 4 CONCLUSIONS

1) In as-cast and homogenized Ti-xZr samples,  $\alpha$ -phase was identified by XRD.

2) Microstructure properties observed by SEM and OM changed from lamellar structure to needle-like structure with increasing Zr content.

3) From the results of polarization behavior in the Ti-xZr alloys, the corrosion resistance was increased with increasing Zr content.

4) In the passive stability test, current density of homogenized treatment was lower than that of as-cast treatment, and then, significantly decreased with the increasing time due to formation of dense passive film. Also the current density decreased with increasing Zr content.

Consequently, in the Ti-xZr alloys, surface stability for biomaterials increased as Zr content increased.

#### ACKNOWLEDGEMENT

“This work was supported by research funds from Chosun University(2004), KEMCO(2006) and 2<sup>nd</sup> Stage of Brain Korea 21”

#### REFERENCES

- [1] M. Aziz-Kerrzo, K.G. Conroy, A.M. Fenelon, S.T. Farrell, C.B. Breslin, “Electrochemical studies on the stability and corrosion resistance of titanium-based implant materials”, *Biomaterials*, 22, 1531-1539, 2001.
- [2] L.J. Knob, D.L. Olson, “Metals handbook Corrosion”, 13, 669, 1987.
- [3] E. Eisenbarth, D. Velten, M. Muller, R. Thull and J. Breme, “Biocompatibility of  $\beta$ -stabilizing elements of titanium alloys”, *Biomaterials*, 25, 5705-5713, 2004.
- [4] M.A. Khan, R.L. Williams, D.F. Williams, “The corrosion behavior of Ti-6Al-4V, Ti-6Al-7Nb and Ti-13Nb-13Zr in protein solutions”, *Biomaterials*, 20, 631-637, 1999.
- [5] K.L. Wapner, “Implications of metallic corrosion in total knee arthroplasty”, *Clin Orthop*, 271, 12-20, 1991.
- [6] J. J. Park, H. C. Choe, Y. M. Ko, “Corrosion Characteristics of TiN and ZrN coated Ti-Nb alloy by RF-sputtering”, *Materials Science Forum*, 539-543, 1270-1275, 2007.
- [7] D. Kuroda, M. Ninomi, M. Morigana, Y. Kato, T. Yashiro, “Design and mechanical properties of new  $\beta$  type titanium alloys for implant materials”, *Materials Science and Engineering A*, 243, 244-249, 1998.
- [8] A. V. Dobromyslove, V. A. Elkin, *Scripta Materialia*, “Martensitic transformation and metastable  $\beta$ -phase in binary titanium alloys with d-metals of 4-6 periods”, 44, 905-910, 2001.
- [9] H.A. Luckey, Jr F. Kubli, “Titanium alloys in surgical implants”, ASTM publication STP 796-800, 1-3, 1983
- [10] M. Browne, P. J. Gregson, R.H. West, “*Journal of Materials Science*”, 7, 323, 1996.
- [11] L. L. Shreir, “*Corrosion Handbook*”, 1, 3-31, 1979.
- [12] X. P. Jiang, X. Y. Wang, “Enhancement of fatigue and corrosion properties of pure Ti by sandblasting”, *Materials Science and Engineering A*, 429, 30-35.
- [13] Y. Okazaki, M. Ohota, Y. Ito, T. Tateishi, “Corrosion resistance of implant alloys in pseudo physiological solution and role of alloying elements in passive films”, *Journal of Japan Inst Metals*, 59, 229-236.